

## STEP—A Temperature Profiler for Measuring the Oceanic Thermal Boundary Layer at the Ocean–Air Interface

THEODOR C. MAMMEN

*Institut für Meereskunde, Kiel, Federal Republic of Germany\**

NIKOLAUS VON BOSSE

*Salzgitter Elektronik GmbH, Flintbek, Federal Republic of Germany*

(Manuscript received 17 January 1989, in final form 10 October 1989)

### ABSTRACT

A fast measuring system has been designed and built to determine the oceanic thermal microstructure at the ocean–air interface. The system consists of a profiler sonde, which ascends through the uppermost few meters of the ocean with a speed of typically  $1 \text{ m s}^{-1}$  and carries a fast temperature sensor with a time constant of 0.5 ms and a surface detector. The data rate is 8000 measurements per second and the achieved resolution in temperature is 0.01 K. The instrument has been designed for rough off-shore treatment and to avoid any disturbance of the boundary layer during measurements.

Some measurements of the “cool skin” are shown from in situ experiments.

### 1. Introduction

The oceans exert considerable influence on long and short term weather occurrences due to their enormous expanse as well as their tremendous capacity for storing and transporting heat. One of the most important quantities affecting the energy fluxes between ocean and atmosphere and used for the parameterization of these fluxes is the ocean temperature close to the surface.

#### *a. Determination of the sea surface temperature*

Traditionally, sea surface temperature (SST) is measured at a depth of several meters. Measurements of this so-called bulk temperature are carried out as point measurements with the bucket thermometer, the reversing thermometer, or with vertical profiling CTD- and XBT-sondes (e.g., Pickard and Emery 1982). For the latter three types of measurements the ship must be stopped or slowed down, so that these methods are normally used only on weather ships and research vessels. Continuous measurements are done from drifting or anchored buoys or at a ship's cooling water intake. The latter method is used in the “ships of opportunity” program.

Since only few ship and buoy measurements are available compared with the great extent of the oceans, it is difficult to determine an oceanwide field of the sea surface temperature by in situ measurements.

During recent decades the development in satellite remote sensing has brought about a change in the determination of the SST. The signals from infrared detectors are used to compute sea surface temperatures. Infrared radiometers measure the emerging longwave radiation from the ocean surface, which is related to SST by Planck's law. This signal, however, is perturbed by absorption, emission and scattering processes in the atmosphere and thus needs appropriate corrections. If in situ measurements of the bulk temperature are used for the derivation or validation of these corrections a systematic error may occur, because the detected infrared radiation is emitted only from the top microns of the ocean (Mc Alister and Mc Leish 1969). Due to the boundary layer effect described below, the temperature in this layer may differ from the bulk temperature by several tenths of a degree kelvin.

The “matchups” between satellite SST and bulk temperature are given rms differences that range from 0.5 to 1.5 K (Mc Clain 1985). These differences are due to both the still uncorrected atmospheric variabilities and the boundary-layer effect. For the use of SST it is necessary to minimize measurement errors to less than  $\pm 0.5 \text{ K}$  (Robinson 1983). Thus a better knowledge of both the strength and the behavior of the thermal boundary layer would improve the application of satellite-derived SST.

\* Present affiliation: Deutscher Wetterdienst, Offenbach, FRG.

*Corresponding author address:* T. C. Mammen, Institut für Meereskunde, Kiel, Federal Republic of Germany.

### b. The thermal structure of the upper ocean

A typical vertical temperature distribution of the ocean is shown in Fig. 1: The deep ocean temperature remains nearly constant whereas the temperature in the mixed layer varies due to atmospheric influences. At a distance of about 1 mm from the surface the mixed layer changes into the laminar layer. Transition and laminar layer form the boundary layer. Wind stress, surface tension and energy fluxes between atmosphere and ocean are the main physical processes that lead to the temperature profile in the boundary layer.

#### 1) WIND STRESS

The atmospheric wind exerts a shear stress on the water surface that produces waves at the surface and turbulence below. The latter is a very effective transport mechanism for heat and mass.

#### 2) SURFACE TENSION

Directly at the surface the turbulence is hindered by surface tension. Since surface tension is strong compared to the forces exerted by turbulence elements, the rigid wall approximation may be applied, i.e., the turbulence elements cannot reach the surface. This results in a laminar boundary layer where the transport is governed by diffusion processes. The surface tension not only restricts motion, but it can also induce particle movement at the surface. This happens when surface slicks or horizontal temperature differences cause horizontal variations in surface tension (Marangoni effect; Katsaros 1980). Surface slicks occur when organic or anorganic material is concentrated in patches on the surface or substances are not homogeneously dissolved.

#### 3) ENERGY FLUXES

Beside the motions at the surface, energy fluxes play a key role for development of the temperature distribution. The heat flux between the surface and the deeper ocean must balance the fluxes of net solar and longwave radiation and latent and sensible heat between ocean and atmosphere. The main energy source is the solar radiation. About 93% (Payne 1972) of in-

coming solar radiation at the surface penetrates to several tens of meters depth depending on turbidity. The net longwave radiation is the sum of absorbed downwelling atmospheric radiation and the radiation emitted by the surface. Both processes take place to an amount of 90% in the top 20  $\mu\text{m}$  of the water. This flux is normally directed from the surface to the atmosphere. Its amount decreases with increasing cloud cover and cloud base temperature. It can even be reversed when the cloud base temperature exceeds the SST. The fluxes of latent and sensible heat between atmosphere and ocean act directly at the surface. Their magnitude depends on wind speed, air temperature, dewpoint and water temperature. The fluxes are usually parameterized by the bulk formulae, which use the bulk temperature of the ocean. For future use of these algorithms in combination with satellite-derived data of SST, the difference between surface and bulk temperature is important. Since infrared remote sensing of the SST is restricted to cloud-free areas, the differences are expected to be large: a cloud-free sky allows for maximum net longwave flux from the ocean to the atmosphere, causing a strong cooling of the surface (see below). Usually, the sum of net longwave radiation and of latent and sensible heat fluxes is directed from the ocean to the atmosphere. At night when there is no solar radiation to compensate this flux a strong temperature gradient must exist in the oceanic laminar layer to maintain the heat flux from mixed layer to surface, because the molecular diffusion coefficient is much less than the turbulent one. This leads to the so-called "cool skin" of the ocean (Fig. 1).

### c. Parameterizations and models of the thermal boundary layer

Several authors parameterize the temperature difference using surface wind, observed heat flux, etc. Three models can be distinguished which describe the temperature distribution in the oceanic boundary layer.

#### 1) STAGNANT FILM MODEL

The stagnant film model consists of two layers. In the top layer, the stagnant film, the vertical transport is purely molecular whereas outside this layer the transport is turbulent with an infinite turbulent transport coefficient. The temperature difference in the stagnant film is parameterized by the total energy flux and the wind speed (Hasse 1971; Wu 1984).

#### 2) DIFFUSION MODEL

The diffusion model is based on works by Reichard (1940), see Hasse (1971), on flow pattern at solid walls. He assumed that the turbulent diffusion coefficient is a function of the distance from the wall, i.e., the efficiency of turbulent transport decreases approaching the wall. With known heat flux and a function for the tur-

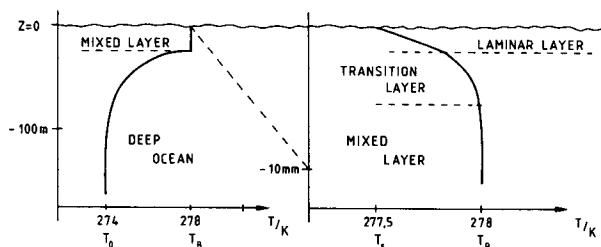


FIG. 1. Schematic ocean temperature profile:  $T_0$  deep ocean temperature,  $T_B$  mixed layer or bulk temperature,  $T_s$  surface or skin temperature.

bulent heat diffusion coefficient, the temperature distribution can be calculated (Hasse 1971; Coantic 1986).

### 3) SURFACE RENEWAL MODEL

The surface renewal model is based on the action of single turbulence elements. It is assumed that a fluid parcel at the surface is completely replaced by a parcel with bulk temperature after a certain time. The time the parcel stays at the surface is related to the intensity of the turbulence. Liu and Businger (1975) applied this model for free surfaces.

All models need measurements for their verification, especially the rigid-wall approximation must still be confirmed. There is need for a three-dimensional temperature field—from the surface to several tens of millimeters depth—measured under natural conditions. Up to now, no technique is available to provide these data, but several attempts have been made to get at least some of them.

#### *d. Measurements of the thermal boundary layer*

In situ measurements in the free ocean are necessary, since some of the important factors like the turbulence structure or natural biological conditions are difficult to establish in a laboratory.

Two measuring systems can be distinguished, the two-point and the profile method.

#### 1) THE TWO-POINT METHOD

This method is based on two measurements: one is carried out as close as possible to the surface and a second one far below the boundary layer ( $>50$  mm). Earlier measurements of this kind were made by Woodcock and Stommel (1946) in shallow water ponds on Cape Cod, Massachusetts. They used thin glass thermometers for both measurements and found temperature differences from  $-0.5$  to  $-1.0$  K between the surface and a depth of  $0.2$  m. Nowadays the upper temperature is usually determined by radiometer measurements made from a ship, while the bulk temperature is measured with relatively slowly responding resistance thermometers positioned in some ten millimeters to m depth. Among others Grassl (1976) used a Barnes PRT-5 infrared radiometer and a PT 100 fixed in  $50$  mm depth by a float. For conditions with solar radiation less than  $200 \text{ W m}^{-2}$  he found a mean difference of  $-0.2$  K. To infer the temperature between both points, models like the aforementioned diffusion or surface renewal model must be applied.

#### 2) THE PROFILE METHOD

With the profile method the vertical temperature profile in the boundary layer is measured with fast-responding thermometers, as was done by Khundzhua

and Andreyev (1974); see also Khundzhua et al. (1977). They used a fast thermocouple thermometer with analog recording on a storage oscilloscope. The sensor was moved from above through the surface with an elevator, fixed to a buoy moored in the Black Sea, at a speed of  $0.17 \text{ m s}^{-1}$ . They approximated the measured mean profile by an exponential function. The mean temperature difference throughout the boundary layer was  $-0.9$  K and the thickness of the boundary layer was  $2$  mm. It is not yet known how these values depend on wind and heat fluxes. Robinson (1984) published some field measurements under various and partly extreme conditions. The range of the temperature difference between surface and bulk extends from  $-3.4$  to  $+5.0$  K. Typical values for the free ocean are expected to range from  $-1.0$  to  $0$  K.

We conclude that there is still a considerable deficit in knowledge about the shape of the vertical temperature profile in the boundary layer. Especially its dependence on surface wind and heat fluxes is largely unknown. More measurements in a free ocean with undisturbed conditions are needed. Such data would improve model verification and as well the matching of bulk and satellite derived SST.

STEP, the Skin-TEmperature-Profiler, is designed to make a step toward these requirements. This system is able to measure the vertical temperature profile in the oceanic boundary layer under nearly undisturbed conditions. The present installation of the equipment, however, restricts the applicability to shallow water ( $<50$  m).

## 2. The method

In order to determine the temperature profile in the aqueous boundary layer under natural conditions, some essential criteria must be satisfied by the measuring system:

(i) *Nondisturbance of the boundary layer.* The measuring device must be designed in such a way that its influence on the conditions that lead to the boundary layer is negligible.

(ii) *High spatial and temporal resolution of the instruments.* The vertical resolution must be sufficient to judge the applicability of existing theoretical models or to develop new ones if needed. Assuming horizontal isotropy, the lack of horizontal resolution may be compensated by a high temporal resolution, i.e., the system must be able to perform repeated measurements at the same place.

(iii) *Reliable location of the measured profile relative to the surface.* The system must allow for the determination of the exact distance between the measurements and the water surface. If a moving system is used, a device is needed to transform the measured time series of the temperature into a scaled vertical profile with a fixed surface level.

(iv) *Robust instrumentation for rough environmental conditions.* Because the system will be used on the open sea, it must be possible to handle the instrument under rough conditions without damage.

To meet these criteria, a completely new measuring system is necessary. The instrument described here is an upward profiling buoyancy-driven profiler, carrying a small fast-response temperature sensor and a surface sensor. The data logging is done on line with a processing unit.

#### a. Upward profiler

Contrary to the more common dropsonde, the STEP-system is released below the surface and rises buoyancy-driven to the sea surface. This method has several advantages.

##### 1) NO DISTURBANCE OF THE ENVIRONMENTAL CONDITIONS

The environmental conditions in the air and in the water adjacent to the surface are very important for the generation of the thermal boundary layer. Since the upward profiler can work at a distance of more than 100 m from the ship, the natural conditions of wind, temperature, humidity, radiation and turbulence are not disturbed until the measurement of one profile is finished. After the measurement, the sonde is brought several meters below the surface and is held there until the former balance is restored.

##### 2) SMALL AMPLITUDE OF THE SIGNAL

If the sensor rises into the boundary layer after starting some meters below, the expected temperature difference is about 1 K. When dropsondes fall from the atmosphere into the water, this difference is usually much larger. Due to the limited temporal resolution of thermometers the temperature jump between air and water might conceal the small temperature difference within the boundary layer.

##### 3) CONSTANT FLOW CONDITIONS AROUND THE THERMOMETER

A good temporal resolution of a thermometer requires an optimal heat transfer between sensor and fluid. If the thermometer passes the boundary layer from above, a sudden change in fluid characteristic occurs. To allow an optimum time constant of the thermometer, however, constant flow of water around the sensor and the corresponding heat flux must be established. For dropsondes this is usually well below the boundary layer. Moreover, the heat exchange might be severely hindered by a gas film that surrounds the sensor.

#### b. Fast response temperature sensor

The temperature boundary layer is typically about 0–5 mm thick with a temperature difference up to a few tenths of a degree Kelvin. To resolve the profile, a spatial resolution of about 0.2 mm and a temperature resolution  $\delta T$  of approximately 0.01 K are required. On the other hand, reverse flushing by surface waves must be avoided. The ascent speed of the sonde must therefore always be greater than the vertical speed of the surface caused by waves. We can get an estimate of this speed if we assume a sinusoidal shape of the wave and a maximum steepness of 1/7 (Neumann 1952). Waves with an amplitude of less than 0.5 m create a maximum particle speed of about  $1 \text{ m s}^{-1}$ .

Extremely high requirements are thus imposed on the time constant of the temperature probe and on the sampling rate.

To get a rough estimate of the time constant  $\tau$ , we assume a linear gradient  $a$  between the surface and the mixed layer. The gradient is then given by

$$a = \Delta T / \Delta z \quad (1)$$

where  $\Delta T$  is the temperature difference between surface and mixed layer and  $\Delta z$  the thickness of the laminar layer.

The sonde passes this layer in the time  $\Delta t = \Delta z / v$ , where  $v$  is the sonde speed. We define a temporal temperature gradient  $b$  by

$$b = \Delta T / \Delta t = \Delta T \cdot v / \Delta z \quad (2)$$

where  $\Delta t$  is the time the thermometer is within the laminar layer.

The thermometer follows the temperature change with some delay. Lieneweg (1975) solved this problem for thermometers with exponential behavior, which can be assumed for a cylinder normal to the flow. For  $\Delta t \gg \tau$  he got

$$\Delta T' = b \cdot \tau \quad (3)$$

where  $\Delta T'$  is the temperature difference between thermometer and surrounding fluid,  $b$  the above defined temperature gradient, and  $\tau$  the time constant of the thermometer.

To retrieve an exact measurement of the water temperature, the difference  $\Delta T'$  must be held equal to or less than the thermometer resolution  $\delta T$ .

$$b \cdot \tau \leq \delta T \quad (4)$$

With values of  $v = 1 \text{ m s}^{-1}$ ,  $\Delta T = 0.1 \text{ K}$ ,  $\delta z = 3 \text{ mm}$  and  $\delta T = 0.01 \text{ K}$  we get from (4)  $\tau \leq 0.3 \text{ ms}$ .

In reality, the shape of the profile will differ from the linear one, but the above approximation should give at least the magnitude of the required time constant. From the above equations, it follows also that an adequate spatial resolution of the temperature pro-

file requires a sampling rate corresponding to at least one-half the sensor time constant.

Fast in situ temperature measurements are made with thermistors or resistance thermometers. Embedded thermistors are too slow. Time constants reach only 20 ms (Lueck et al. 1977). Platinum film thermometers are available with very short time constants, but they proved unsatisfactory for boundary layer research in the ocean because of their fragility and tendency to loose calibration, as shown in experiments by Frey (1973) and Mammen (1983). Resistance thermometers like the conventional Pt 100 probe are too slow and too large, but with some modifications stable and sufficiently fast responding resistance thermometers can be built (Kroebel and Bosse 1982). The basic idea is to reduce the time constant by eliminating all insulation from the thermometer wire. To avoid measuring errors due to the electrical conductivity of water, the thermometer should have a very low resistance (typically a few m $\Omega$ ). This can be accomplished by a short, thin platinum wire. The loss of resolution due to the small resistance can be compensated by resistance transformation (Kroebel 1980). Such a transformer acts like an amplifier but without generating any noise.

The time constant of a platinum wire can be calculated similar to a cylinder, which is in a flow normal to its axis. For this problem Lieneweg (1975) gives the equation

$$\tau = Rc\rho/\alpha \quad (5)$$

where  $R$  is the radius of the wire,  $c$  is the heat capacity and  $\rho$  is the density of the thermometer material. The convection heat transfer coefficient  $\alpha$  can be calculated from the flow properties like viscosity  $\nu$ , thermal diffusivity  $a$ , thermal conductivity  $h$  and the probe diameter  $D$  with the nondimensional Nusselt number  $Nu = \alpha D/h$ , Prandtl number  $Pr = \nu/a$  and Reynolds number  $Re = vD/\nu$  (Incropera and Witt 1981). A relation is given by Kramers; see Corrsin (1963):

$$Nu = 0.42 Pr^{0.2} + 0.57 Pr^{0.33} Re^{0.5} \quad (6)$$

This gives for  $\alpha$

$$\alpha = \frac{h}{D} (0.42 Pr^{0.2} + 0.57 Pr^{0.33} Re^{0.5}) \quad (7)$$

Using Eq. (5) and (7), the required diameter of the wire can be calculated. To achieve a time constant of 0.5 ms at a flow speed of 1 m s<sup>-1</sup> the diameter of the wire must be not more than 0.05 mm.

### c. Surface sensor

Preliminary investigations by the authors have shown that for a reliable evaluation of measured tem-

perature profiles an independent measurement of the position of the water surface and the speed of the sonde relative to the surface is necessary. Attempts to determine the surface position using the sudden temperature change when emerging from the surface of the water proved to be unreliable, because the conditions in the layer above the water surface do not always enable heat transport.

Therefore, a new sensor, a so-called surface detector, was constructed which reliably recognizes the surface of the water and allows measurement of the speed of the thermometer when moving through the surface layer. The detector monitors the seawater-induced short circuit between a pair of electrodes located at some distance from the thermometer. The interruption of the short circuit determines the event of surface penetration. If the vertical distance between the surface sensor and the temperature probe is known, the exact position of the surface penetration on the temperature profile can be determined (Fig. 5). To measure the speed of the sonde, the same measurement is made on the opposite side of the temperature sensor with a second pair of electrodes with some offset in height. From

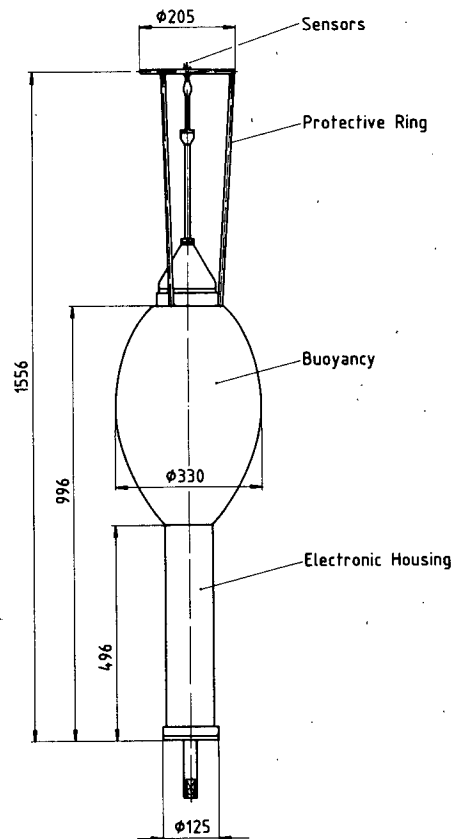


FIG. 2. Schematic drawing of STEP. The electronic housing is made of stainless steel. The weight is 250 N and the net buoyancy force is 130 N. The dimensions are in mm.

the two measurements the penetration speed can be calculated (section 4).

### 3. The measuring system

To measure the temperature profile in the oceanic boundary layer at the ocean-atmosphere interface, a completely new measuring system has been developed. The system consists of an upward profiler with a fast-response thermometer, a surface and speed detector, and an on-line data transmission and recording system.

The profiler is shown schematically in Fig. 2. The instrument is 1.996 m long. The total weight of 250 N is nearly all centered below the buoyancy body. The displacement under water is 380 N. So a net buoyancy force of 130 N results. All parts of the profiler are designed to obtain a low drag coefficient (approximately 0.9). In shallow water with a depth to 50 m the profiler is moved over a block moored at the ground (Fig. 3). The profiler can be pulled under water with a thin rope using a small winch on board the ship. When the rope is released, the profiler rises to the surface with a maximum speed of  $2.5 \text{ m s}^{-1}$ . If the ascension speed is reduced to  $1 \text{ m s}^{-1}$  with the winch, a net buoyancy force of 107 N still remains and leads to a steady movement up to the surface.

The sensors are located at the top of the profiler (Fig. 4). They are protected by a ring which is wide enough to avoid any disturbance of the surface before the sensors have reached it. The sensors are about 10 mm above the protection ring. The distance between the sensors and the buoyancy body is kept large enough to guarantee that the effects of the flow induced ahead of the buoyancy body are small compared to the spatial resolution of the temperature and surface measurement. All parts of the profiler are slender and smooth.

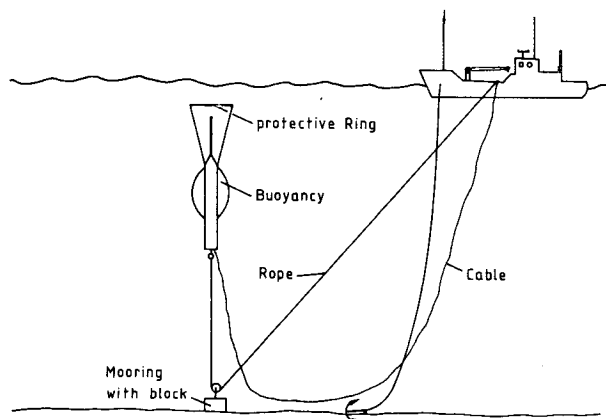


FIG. 3. Schematic drawing of the system during in situ measurements in shallow water.

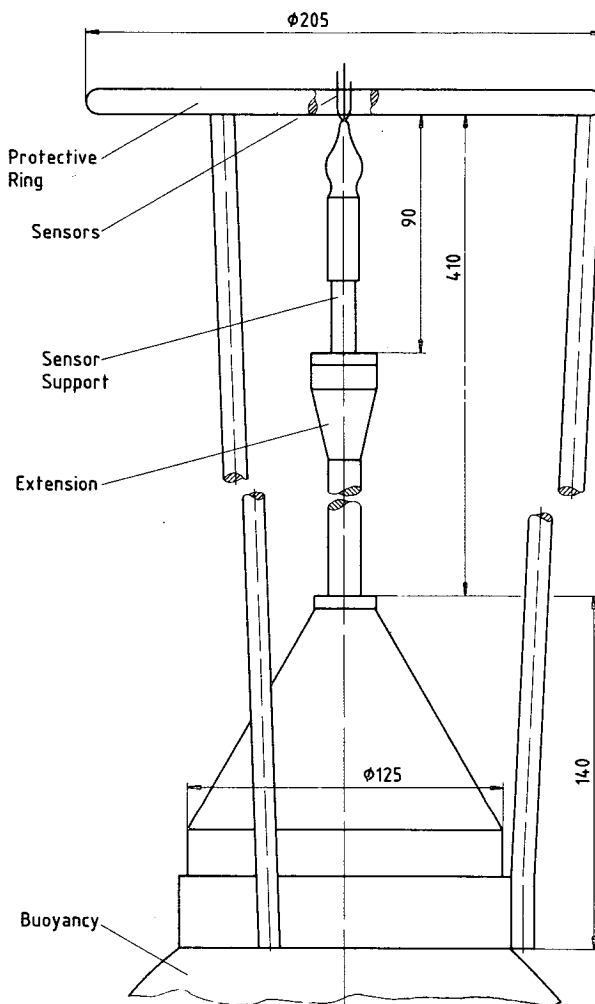


FIG. 4. The upper part of STEP. The protective ring, the sensor support and the extension are made of stainless steel.

Figure 5 shows the sensors in detail. The temperature sensor is a platinum wire approximately 2 mm long and 0.05 mm in diameter welded to the ends of two 0.2 mm-thick platinum wires. These wires are insulated and fasten the sensor at a distance of 20 mm from the holder. The time constant of the sensor is 0.5 ms at a flow velocity of  $1 \text{ m s}^{-1}$ .

An ac voltage is generated from the very small thermometer resistance by means of an ac current source. With a transformer the signal can be increased to a sufficiently high level to be amplified by a low-noise amplifier. The output signal is then treated using the two-phase-bridge technique (Kroebel 1974), a method to convert sinusoidal bridge signals to digital values. In order to achieve a sufficiently high data rate, we modified the two-phase bridge so that it was possible to use a sine wave with a higher frequency of 8 KHz and a system cycle of 65 MHz. Our noise reduction was so successful that it was no longer necessary to

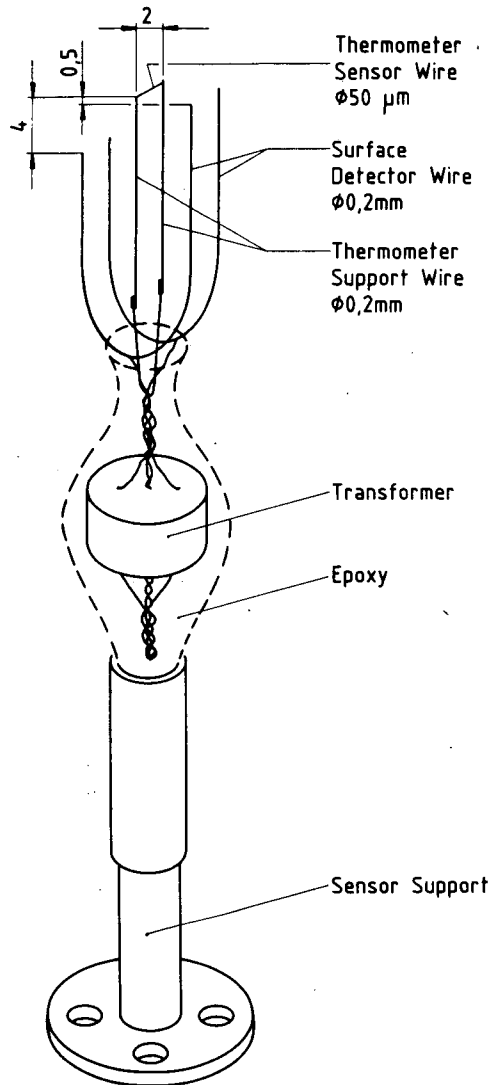


FIG. 5. The Schematic view of the temperature sensor and the surface detector.

calculate average values in order to get stable results at high data rates. The system provides a 13-bit value with a rate of  $8000 \text{ s}^{-1}$  and temperature ranges of 5 K can be resolved to 0.01 K.

The surface detector consists of two pairs of 0.2 mm-thick platinum wire electrodes, located about 0.5 mm and 4.5 mm below the temperature sensor, respectively. The wires are insulated except at their tip. The tip diameter of 0.2 mm is sharpened so that a good penetration of the surface can be assumed.

In a bridge circuit the two pairs of electrodes are switched in a series, so that the conductance of the upper and lower pairs of electrodes is measured additively. If the upper pair emerges from the water, the conductance changes suddenly. If the lower pair then also emerges from the water, the conductance changes

drastically once again. This series of measured values is transmitted via a second channel at the rate of the temperature sensor. With a known scanning rate and the above-described geometry, the zero-point and scale of the depth can be determined from the signal.

The data undergoes a parallel-serial transformation within the sonde, so that it can be transmitted by a simple two-wire technique to a computer on the research vessel. Each data cycle consists of two 16-bit words and is transmitted as a set via a 100-m long cable to an 8-bit microcomputer. After decoding into parallel data in a special interface, the measured values are stored in a core memory cyclically, i.e., data is overwritten as soon as the memory (54 Kbytes) is full (Fig. 6).

The signal of the surface detector is continuously monitored and overwriting is stopped as soon as the sensor has left the water. This results in a temperature profile from the surface downward to a depth of approx. 1.7 m (sonde velocity  $1 \text{ m s}^{-1}$ ). During the measuring procedure data is stored on floppy disk and the profile can be plotted on a dot matrix printer.

#### 4. Results

In the following we give examples of some typical measurements. A more extensive dataset will be published later. The system was tested both in the laboratory and in the shallow water of Kiel Bay.

Laboratory tests were carried out in a tank of 1.5 m depth and 1.2 m diameter. Under reproducible environmental conditions like surface energy fluxes and turbulence the instrument worked well.

Examples of measurements taken off the pier of the Institut für Meereskunde in Kiel are shown in Fig. 7–9. The pier is situated at the west shoreline of the Kieler Förde where the Fjord approximately 1 km wide. Figure 7 shows a typical recording of the surface detector. The abscissa is scaled into arbitrary units of conductivity between the two surface detectors, while the ordinate shows cycle numbers of the measured time series. With a given cycle length of 0.125 ms this scale can be transformed either into units of time or with a given vertical distance between the two surface detectors into a depth scale.

The sharp changes in signal indicate penetration of each of the two pairs of surface detectors through the surface. From the number of cycles between penetrations and the known vertical distance between the detectors, the velocity of the sonde relative to the surface can be calculated. With this speed and the distance between one surface detector and the thermometer, the depth scale of the temperature signal is computed.

The temperature profiles shown in Figs. 8–9 were taken under clear sky conditions at night (no solar radiation). The outgoing longwave radiation computed by the Stefan-Boltzmann law overcompensated with  $320 \text{ W m}^{-2}$  the measured downwelling atmospheric

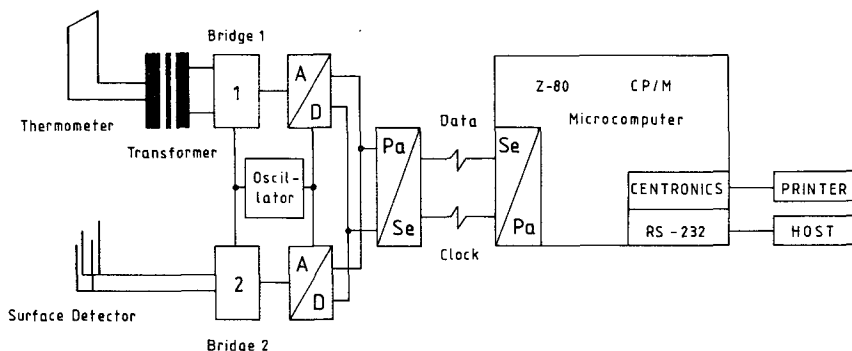


FIG. 6. Block diagram of the electronic part of the STEP system.

radiation of approximately  $220 \text{ W m}^{-2}$ , resulting in a net radiation loss of the ocean surface of approx.  $100 \text{ W m}^{-2}$ . The latent and sensible heat fluxes was calculated by the bulk formulae. Since the formulae were developed for the free ocean, they give only a rough estimate of the fluxes in the case of a short fetch. The free parameters were set according to Isemer (1987). With easterly winds of  $3 \text{ m s}^{-1}$  the mean sum of latent and sensible heat flux was about  $-25 \text{ W m}^{-2}$ . This results in a net energy flux of about  $125 \text{ W m}^{-2}$  directed from the ocean into the atmosphere.

Figure 8 shows a typical temperature profile in the boundary layer measured at the pier. Because the temperature at the surface is less than it is several millimeters below, the heat flux is directed upwards from the mixed layer to the surface. As the shape of the curve may be influenced by the limited temporal resolution of the thermometer, a correction is applied. For this purpose a third-order polynomial is fitted to the original data of the boundary layer by the least

squares method (solid line). The resulting rms is of the same order of magnitude as the electronic noise. Then a recursive filter in the time domain (Fozdar 1985) is applied to this function (dotted line). The time constant used is computed from the sonde speed by Eqs. (5), (6) and (7). Then the unsmoothed data are corrected with the difference between the corrected and original but smoothed function at every depth. This leads to a temperature profile with the influence of the thermometer time constant eliminated. The advantage of the method is that no noise is amplified.

As mentioned in section 1, the heat flux in the boundary layer takes place only by molecular diffusion, which results in an approximately linear temperature profile in the uppermost part of the profile. Thus, the heat flux can be calculated from the constant temper-

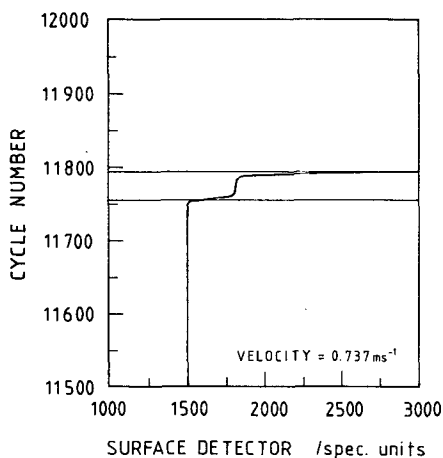


FIG. 7. Typical signal of surface detectors recorded in situ. The values on the abscissa are proportional to the conductivity between the sensing elements. The ordinate is scaled in units of time.

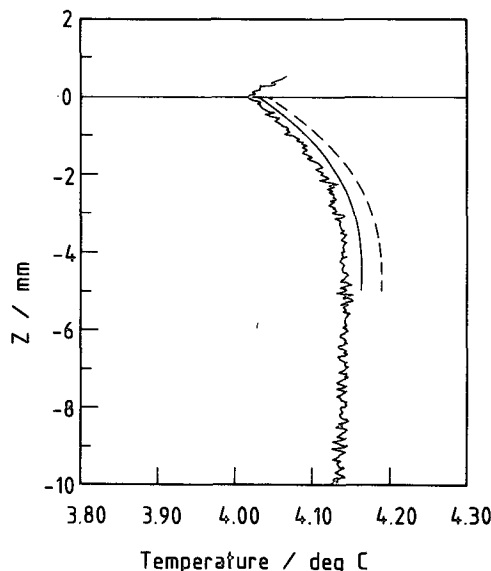


FIG. 8. Temperature profile measured in Kieler Förde at the pier of the Inst. f. Meereskunde. Solid line: fitted polynomial. Dashed line: function after time constant correction. (Lines are shifted by  $0.025 \text{ K}$ .)



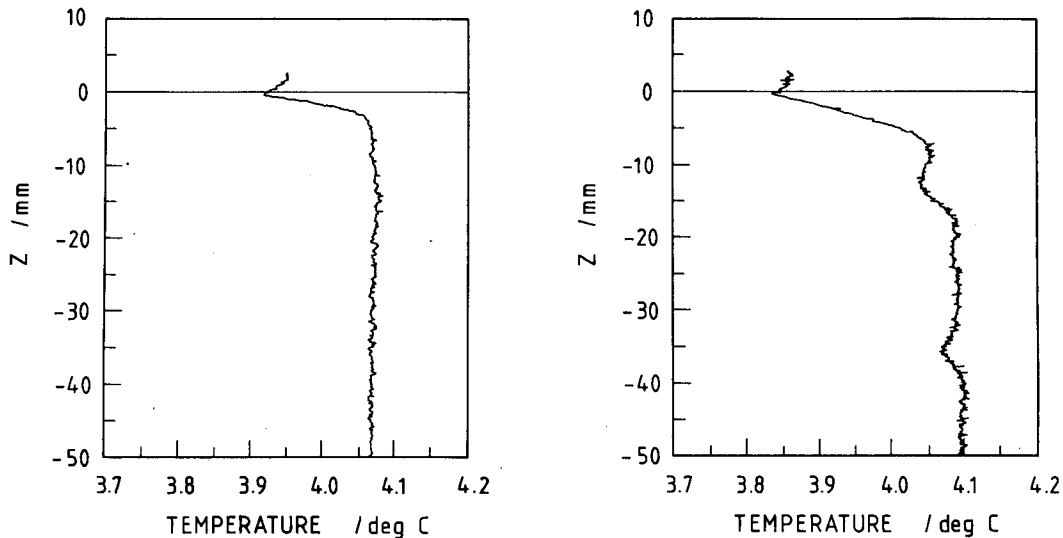


FIG. 9a,b. Temperature profiles measured in Kieler Förde at the pier of the Inst. f. Meereskunde (Net heat flux approx.  $-125 \text{ W m}^{-2}$ ).

ature gradient in this layer using the thermal diffusion coefficient. The calculation gives  $-35 \text{ W m}^{-2}$  in this case which is typical for this situation and somewhat different from the mean net energy flux of  $-125 \text{ W m}^{-2}$ .

Two more examples of measured temperature profiles down to a depth of 50 mm are shown in Figs. 9a and b. The heat fluxes calculated from the linear part of the profiles are  $-75$  and  $-45 \text{ W m}^{-2}$ . Figure 9a shows the exponential shape of the profile in the boundary layer and a constant temperature in the mixed layer. If the temperature jump increases, unstable layering will result and the water at the surface will

be mixed with water of lower layers by convection. Variations of the temperature signal in Fig. 9b show some convection cells. Several profiles were taken under almost the same conditions and show similar processes with various temperature differences between the surface and the mixed layer.

The limitation of the system with respect to resolution can be seen in Fig. 10. This measurement was taken from a research vessel about 0.5 km offshore. Obviously, a very sharp temperature gradient occurs in the upper 0.5 mm. At a vertical sonde speed of  $1.1 \text{ m s}^{-1}$  this layer was passed within 0.5 ms, which is on the order of magnitude of the thermometer time constant. The sampling rate of 8 kHz allows only four measurements in this layer. Thus the comparison with theoretical profiles, the fitting of the polynomial and the calculation of the heat flux may be inaccurate.

The difference between the traditionally calculated mean net energy flux and the heat fluxes computed from the measured temperature profiles may have different reasons. Besides uncertainties in the measurements of the environmental data and the parameterizations used for the mean energy fluxes, the limited temporal resolution of the system may cause heat fluxes that are too small because very thin boundary layers with a strong temperature gradient are not resolved. Such profiles would result in stronger heat fluxes.

Besides the measurements shown in this paper a large number of profiles with the corresponding meteorological data to calculate mean heat fluxes have been recorded from research vessels in Kiel Bay under different heat fluxes and wind speeds up to  $10 \text{ m s}^{-1}$  with the accompanying waves.

Precise statements about the behavior of the boundary layer cannot be made until the current evaluations have been completed.

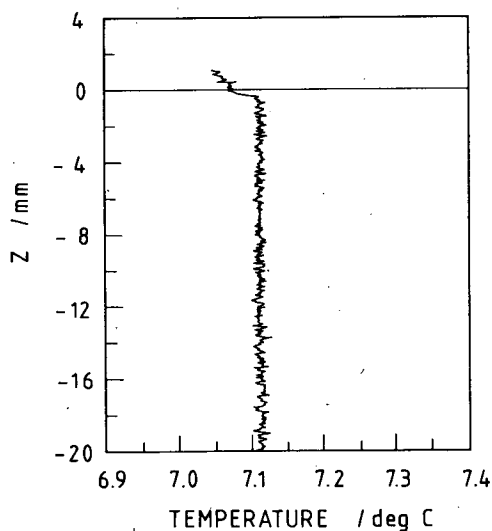


FIG. 10. Temperature profile recorded about 0.5 km from the shore with an offshore wind of  $10 \text{ m s}^{-1}$  and a net heat flux of  $-100 \text{ W m}^{-2}$ .

## 5. Summary and discussion

We demonstrated a new approach to the measurement of the "cool skin" of the ocean. Following the basic idea of upward profiling we have shown that a complete new system consisting of a fast temperature probe and a surface detector along with high speed data recording is necessary to measure meaningful temperature profiles in the boundary layer.

Four problems needed to be solved.

### a. Fast response resistance thermometer

We used a thin platinum wire of 50  $\mu\text{m}$  diameter mounted on two 0.2 mm thick platinum wires. Its time constant was approx. 0.5 ms at a flow speed of 1 m  $\text{s}^{-1}$ . Experience has shown that this sort of thermometer is very robust and that the diameter could be reduced to achieve an even smaller time constant. This is necessary to resolve laminar layers thinner than 0.5 mm.

### b. Vertical scaling of the temperature profile

A new device, the so-called surface detector, has been constructed. With this method it has been possible to match the temperature profile with a depth scale relative to the moving surface. The surface detector used in the system permits a calculation of the depth scale with an accuracy of about 0.2 mm. For this calculation it must be assumed that the relative velocity between surface and sonde is constant while the two detectors penetrate it.

### c. Analog electronics and A/D converter

A sophisticated transformer technique together with a carefully designed low noise AC-bridge has lead to a suitable resolution (better than 0.01 K). The achieved data rate of 8000  $\text{s}^{-1}$  might be increased by using modern fast A/D converters. This will be needed to get at least ten measurements in the laminar layer to fix an appropriate mathematical function even under conditions when the layer is very thin.

### d. Digital data processing

In general data handling from oceanic sondes has been achieved in two ways:

- short time data storage inside the sonde and subsequent retrieval of the data when aboard ship
- on-line data transmission to a recording device on board the vessel.

We used the latter method because the system should be able to work continuously over several hours without disturbing the upper ocean by mechanical mixing. With our sonde, series over several tens of hours long can be recorded. The first method may become feasible for

future deep ocean application since RAM chips with greater storage capacity are now available.

In section 2 the design requirements for the optimum measuring system were formulated. With the system presented in this paper we have met all of them. Calculations have shown that the expected shape of temperature profiles can be reproduced and heat fluxes calculated for laminar layers thicker than 0.5 mm.

Taking the experiences up to the present into account, a measuring system that is able to determine the temperature profile in a moving boundary layer in situ has been successfully developed. Further improvements are possible.

*Acknowledgments.* We would like to acknowledge Prof. L. Hasse and Dr. C. Simmer for all the useful discussions and F. Nevoigt, who prepared the figures. We are grateful to P. Timm and several students as well as the crews on the research vessels of the Institut für Meereskunde for their assistance in data collection.

This study will be part of the Ph.D. thesis of T. Mammen and was supported by the Deutsche Forschungsgemeinschaft under SFB 133/B2.

## REFERENCES

- Coantic, M., 1986: A model of gas transfer across air-water interface with capillary waves. *J. Geophys. Res.*, **91**, 3925-3943.
- Corrin, S., 1963: Turbulence: Experimental methods. *Flügge: Handbuch der Strömungsmechanik*. Springer Verlag, 696 pp.
- Fozdar, F. M., G. J. Parker and J. Imberger, 1985: Matching temperature and conductivity sensor response characteristics. *J. Phys. Oceanogr.*, **15**, 1557-1569.
- Frey, H. R., and G. J. McNally, 1973: Limitations of conical hot platinum film probes as oceanographic flow sensors. *J. Geophys. Res.*, **78**, 1449-1461.
- Grassl, H., 1976: The dependence of the measured cool skin of the ocean on wind stress and total heat flux. *Bound.-Layer Meteor.*, **10**, 465-474.
- Hasse, L., 1971: The sea surface temperature deviation and the heat flow at the sea-air interface. *Bound.-Layer Meteor.*, **1**, 368-379.
- Incropera, F. P., and D. P. de Witt, 1981: *Fundamentals of Heat Transfer*. Wiley and Sons, 819 pp.
- Isemmer, H. J., 1987: Optimierte Parametrisierungen der klimatologischen Energie- und Impulsflüsse an der Oberfläche des Nordatlantik. Ber. d. Inst. f. Meereskunde 160, Kiel, Düsternbrooker Weg 20.
- Katsaros, K., 1980: The aqueous thermal boundary layer. *Bound.-Layer Meteor.*, **18**, 107-127.
- Khundzhua, G. G., and Y. G. Andreyev, 1974: An experimental study of heat exchange between the ocean and the atmosphere in small-scale interaction. *Izv. Atmos. Oceanic Phys.*, **10**, 1110-1113.
- , A. M. Gusev, Y. G. Andreyev, V. V. Gurov and N. A. Skorokhvatov, 1977: Structure of the cold surface film of the ocean and heat transfer between ocean and atmosphere. *Izv. Atmos. Oceanic Phys.*, **13**, 506-509.
- Kroebel, W., 1974: A two phase bridge as a basis for in situ measurements of differential physical parameters. *Ocean 1974*, **1**, 178-180.
- , 1980: Über einen Temperaturfühler hoher Auflösung und einer Zeitkonstante von 1 . . . 1.5 ms für In-situ-Anwendungen in der Ozeanographie und auf anderen Gebieten. *Atomenerg.-Kerntech.*, **36**, 102-106.

- , and N. v. Bosse, 1982: Progress in oceanographic high speed resistance thermometry and applications in a new temperature gradient- and turbulence-meter. OCEANS '82, IEEE Publ. No. 82CH1827-5, Washington, DC, 272-276.
- Lieneweg, F., 1975: *Handbuch der Technischen Temperaturmessung*. Vieweg-Verlag, Braunschweig.
- Liu, W., and J. A. Businger, 1975: Temperature profile in the molecular sublayer near the interface of a fluid in turbulent motion. *Geophys. Res. Lett.*, **2**, 403-404.
- Lueck, R. G., O. Hertzmann and T. R. Osborn, 1977: The spectral response of thermistors. *Deep-Sea Res.*, **24**, 951-970.
- Mammen, T., 1983: Zur Messung der Temperaturgrenzschicht im Wasser an der Grenzfläche Ozean-Atmosphäre. Diplomarbeit im Fachbereich Mathematik-Naturwissenschaften der Christian-Albrechts-Universität Kiel.
- Mc Alister, E. D., and W. Mc Leish, 1969: Heat transfer in the top millimeter of the ocean. *J. Geophys. Res.*, **74**, 3408-3414.
- Mc Clain, E. P., W. G. Pichel and C. C. Walton, 1985: Comparative performance of AVHRR-based multichannel sea surface temperatures. *J. Geophys. Res.*, **90**, 11 587-11 601.
- Neumann, G., 1952: Über die komplexe Struktur des Seeeganges. *Dtsch. Hydr. Z.*, **5**, 252-277.
- Payne, R. E., 1972: Albedo of the sea surface. *J. Atmos. Sci.*, **29**, 959-970.
- Pickard, G. L., and W. J. Emery, 1982: *Descriptive Physical Oceanography*. Pergamon, 249 p.
- Robinson, I. S., N. C. Wells and H. Charnock, 1984: Review article: The sea surface thermal boundary layer and its relevance to the measurement of sea surface temperature by airborne and spaceborne radiometers. *Int. J. Rem. Sens.*, **5**, 19-45.
- Woodcock, A. H., and H. Stommel, 1947: Temperatures observed near the surface of a fresh water pond at night. *J. Meteor.*, **4**, 102-103.
- Wu, J., 1984: On the cool skin of the ocean. *Bound.-Layer Meteor.*, **31**, 203-207.